

Paper 5-3 has been designated as a Distinguished Student Paper at Display Week 2025. The full-length version of this paper appears in a Special Section of the *Journal of the Society for Information Display (JSID)* devoted to Display Week 2025 Distinguished Papers. This Special Section will be freely accessible until December 31, 2025 via:

<https://sid.onlinelibrary.wiley.com/doi/full/10.1002/jsid.2054>

Authors that wish to refer to this work are advised to cite the full-length version by referring to its DOI:

<https://doi.org/10.1002/jsid.2054>

Highly Efficient and Bright Green Quantum-Rod Light-Emitting Diodes with Eliminated Charge Leakage

Kumar Mallem*, Zebing Liao*, Maksym F. Prodanov*, Meiqi Sun*, Jianxin Song*, Debjyoti Bhadra*, Abhishek K. Srivastava*,&

*State Key Laboratory on Advanced Displays and Optoelectronics Technologies and Centre for Display Research, Department of Electronics and Computer Engineering, The Hong Kong University of Science and Technology, Clear Water Bay, Kowloon, Hong Kong 999077, China

&IAS Center for Quantum Technologies, The Hong Kong University of Science and Technology, Hong Kong, China

Abstract

Quantum rods (QRs) have the potential to double the external quantum efficiency (EQE) of light-emitting diodes (LEDs) compared to traditional spherical quantum dot (QD) LEDs. However, the EQE and brightness need to catch up to those of QD-LEDs. One of the primary factors contributing to this issue is electron leakage and parasitic emission from the hole transport layer (HTL), diminishing the EQE and brightness by over 80%. In this study, we systematically analyzed charge transport behavior in QR-LEDs and identified the pathways for electron leakage. We discovered two primary leakage paths enabling simultaneous electron-hole recombination in the QRs and the HTL. The electroluminescence (EL) spectra indicate that the parasitic emission from the HTL is substantial, accounting for more than 50% of the signal compared to that of the QRs. We enhanced device performance by effectively suppressing electron leakage and improving hole injections in QR-LEDs. As a result, QR-LEDs achieved record-breaking performance metrics: EQE of 19.4%, CE of 72 cd/A, and luminance of 320,000 cd/m². These figures represent the highest recorded values for green QR-LEDs.

Author Keywords

Electron leakage current; parasitic emission; electron-hole recombination; QR-LEDs; charge balance.

1. Introduction

Light-emitting diodes (LEDs) that incorporate colloidal quantum dots (QDs) are becoming increasingly attractive for the future of the display and lighting industry. This interest is driven by their low-cost processability, high efficiency, excellent color purity, low operating voltages, and compatibility with existing display and lighting technologies [1-4]. Over the past decade, significant advancements have been made in QD-LEDs, focusing on the chemical synthesis of QDs, the development of inorganic electron transport layers (ETLs), organic hole transport layers (HTLs), and improvements in device architecture [2-4]. As a result, the external quantum efficiency (EQE) of QD-LEDs has reached its theoretical limit of over 25%, primarily constrained by light outcoupling efficiency (η_{out}), which is ~20%. To improve light η_{out} from the device, several strategies have been suggested. These include changing the flatness of the substrates, refractive index matching, patterned QD layers, and using anisotropic nanocrystals like quantum rods (QRs) as an emissive layer [5-8]. The light that exits the device with isotropic emitters primarily comes from horizontal transition dipole moments (TDM), while vertical TDM contributions are negligible due to light being trapped in surface plasmon modes [7, 8]. Therefore, enhancing the horizontally aligned TDM is the best way to boost the device's light η_{out} . QRs offer a simple solution to surpass the η_{out} of spherical QDs, typically ~0.2, owing to their horizontally aligned in-plane TDMs. This alignment has the potential to double the η_{out}

of LEDs.

Shape geometry of QRs offers several optical advantages over QDs, such as a significant Stokes shift, reduced Förster resonance energy transfer (FRET) due to greater inter-particle distances, high photoluminescence quantum yield (PLQY) in films, and linearly polarized emission [9-12]. A key advantage is that spin-coated QRs often align parallel to the substrate, leading to horizontally aligned TDMs, which could double the device's light η_{out} . However, these benefits were not successfully employed in LED applications. Some efforts have been made to develop efficient red QR-LEDs and a reported peak EQE of only 22% [13] to date [12], significantly below the theoretical limit of 50% and even lower than QD-LEDs. The situation is even worse for green and blue QR-LEDs, which have EQEs of 14.2% [14] and 9.4% [15], as reported by our group recently. This underperformance of green and blue QR-LEDs is primarily attributed to inadequate synthesis techniques for producing high-quality QRs with PLQYs exceeding 90% in the green and blue regions. Additionally, factors such as the uniformity of the rod shape and the composition of the QRs also significantly impact device performance and need to be improved.

In this study, we synthesized green QRs, achieving a PLQY of over 95%, and demonstrated highly efficient, bright, and stable green QR-LEDs by addressing the issue of electron leakage current in the device. Electron leakage into HTL via QRs leads to simultaneous electron-hole recombination in both the HTL and QRs, causing parasitic emission from the HTL that negatively affects device performance and pushing the electron-hole recombination away from the QRs. The electron leakage primarily occurs through two pathways: 1) energetic disorders in the HTL and 2) crossing the energy offset at the HTL/QR interface. We eliminated these leakage paths by modulating HTL and employing device engineering strategies. This approach effectively blocked electron leakage and improved charge balance within the device. As a result, the peak EQE and brightness of the green QR-LEDs reached 19% and 230,000 cd/m², respectively.

2. Results and Discussion

The synthesis process for the green QRs followed our previous method with minor modifications, and we will soon publish the detailed synthesis of the CdSe/Zn_xCd_{1-x}S/ZnS core/gradient alloy structure of the QRs. Figures 1(a) and 1(b) display the morphology of the QRs, confirmed by HR-TEM images; the average length and diameter of the QRs are ~ 22 and 5 nm. The aspect ratio of the QRs is 4.4, suitable for polarized emissions with good alignment. The QRs exhibit a uniform shape throughout, with no strains, and the shape uniformity of the green QRs is significantly better than in our earlier reports. Non-uniformity and strains can adversely affect device performance,

leading to low QY and poor charge injection. Figure 1(c) shows an SEM image of the QRs, where they uniformly dispersed and horizontally aligned spin-coated QRs on the substrate, contributing to a high ratio of horizontally aligned TDMs. Figure 1(d) shows the absorption and emission peaks of the QRs. The emission has a narrower full width at half maximum (FWHM) of 32 nm, with an emission wavelength of 520 nm, placing it well within the color triangle, making it ideal for display applications. The PLQY of the QRs exceeds 95%, highlighting their potential for developing highly efficient and bright LEDs

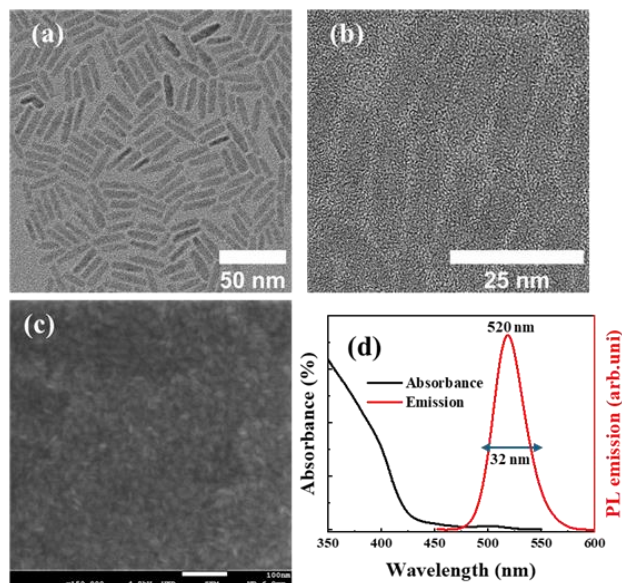


Figure 1. (a) transmission electron microscope (TEM) image of the QRs, and high-resolution (HR-TEM) image in (b), (c) scanning electron microscope (SEM) image of the spin-coated QRs film, and (d) PL absorbance and emission peaks of the QRs.

The fabrication of the QR-LEDs follows a method similar to our previous reports, with the device structure comprising ITO/PEDOT:PSS/TFB/QRs/ZnMgO/Al, as illustrated in Figure 2(a). We selected TFB as HTL due to its deep HOMO level of -5.4 eV and high hole mobility of $1 \times 10^{-3} \text{ cm}^2 \text{ V}^{-1} \text{ s}^{-1}$. This matches well with the electron mobility of ZnMgO, ensuring balanced charge carrier injection into the QRs. The UPS spectra were utilized to measure the HOMO level of the QRs, while the band gap of the QRs was determined from the absorption spectra. Figure 2(b) presents the energy band diagram, illustrating the injection of electrons and holes into the QRs, where they recombine radiatively and emit the photons. Unexpectedly, the QR-LED's EL spectra show a significant parasitic emission from the TFB, as shown in Figure 2(c). This suggests electron leakage and exciton formation in the TFB layer. The TFB parasitic emission is substantial, only 50 % lower than the QRs. This indicates that the QRs are negatively charged with electrons and leak electrons into the TFB layer ($\text{QRs}^- + \text{HTL} \rightarrow \text{QR} + \text{HTL}^-$), enabling simultaneous electron-hole recombination in both the QRs and TFB. Surprisingly, TFB parasitic emission from the device was detected as soon as the device lit up at 2.2 V, confirming that the electron leakage into the TFB even occurred before the device turned on at a more negligible bias. The electron leakage and parasitic emission from the HTL significantly affect the device's performance, including low EQE and high-efficiency roll-off. The electron leakage into the TFB occurs primarily in two paths, as illustrated in Figure 2(b). However, it is challenging

to identify electron leakage paths, as they change the direction of the path with applied voltage.

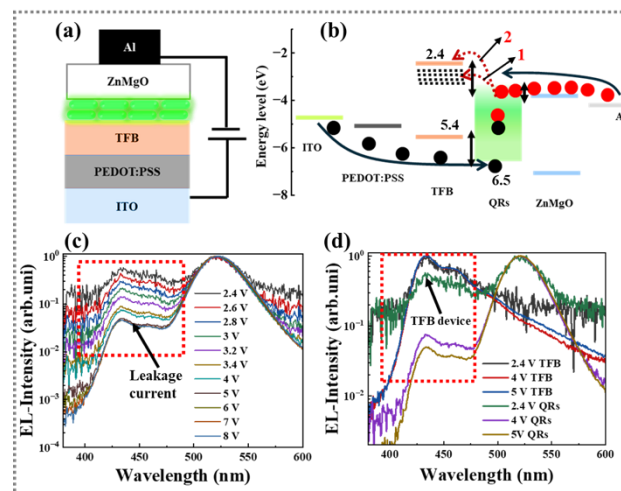


Figure 2. (a and b) Schematic and energy band diagram of the QR-LEDs, (c and d) EL spectra of the device highlighting the electron leakage in the form of TFB parasitic emission, (d) EL spectra of the device QR-LEDs and TFB devices, where the structure of the TFB device is (ITO/PEDOT:PSS/TFB/ZnMgO/Al).

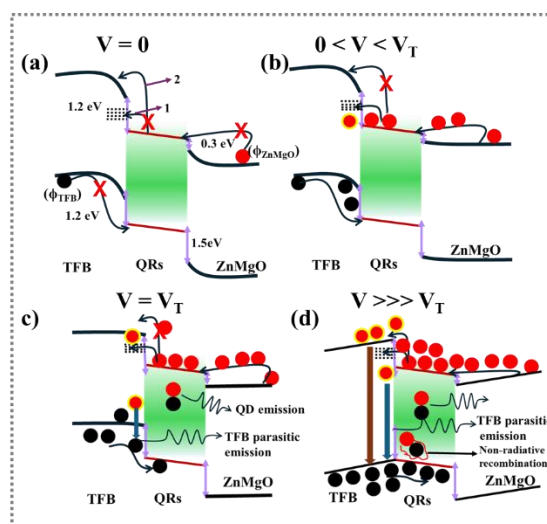


Figure 3. The energy band diagram of the green QR-LEDs at different voltages represents the electron leakage paths into the TFB. (a) $V = 0$, at thermal equilibrium, there is no charge injection, (b) $0 < V < V_T$, the ZnMgO bands become flat, electrons overcome the 0.3 eV injection barrier and enter the QRs. At the same time, the holes are accumulated at the TFB/QRs interface. (c) $V = V_T$, TFB bands also become flat, and both the carriers enter the QRs and radiatively recombine; also, the electrons leak into the TFB via path 1(d) $V \gg V_T$, the electrons leak into the via path 1 and path 2.

Identifying the electron leakage paths.

Figure 3 analyzes the device's charge injection, recombination, and electron leakage paths. When the $V = 0$, there is no current flow at thermal equilibrium, as shown in Figure 3(a), resulting in no leakage current. When V is slightly positive ($0 < V < V_T$,

where V_T is the threshold voltage), the energy bands of TFB and ZnMgO flatten, pushing electrons and holes toward the QR layer, as shown in Figure 3(b). As V increases to 1V, the current rises linearly from the J-V curves due to thermally generated minority carriers. After reaching 1V, the current increases significantly due to the majority of carriers. Electrons enter the QRs much faster than holes because the electron injection barrier at the QR/ZnMgO interface (0.3 eV) is much lower than the hole injection barrier at the TFB/QRs interface (1.2 eV). This results in excess electrons accumulating at the TFB/QRs interface, as illustrated in Figure 3(b). $V = V_T$, both carriers enter the QRs, recombining radiatively and emitting the photons. The EL spectra in Figure 2(c) reveal the TFB parasitic emission from the device at 2.4V; this conforms to the electron-hole recombination in both QRs and TFB shown in Figure 3(c). Electrons leaking QRs to TFB need to overcome the 1.2 eV energy offset between the LUMO of the TFB to the conduction band of QRs, which is considered highly inefficient at an applied slight bias of 2.4 V, while the hole injection barrier from the TFB to the QRs is 1.2 eV. To verify our hypothesis, we constructed a device without QRs (ITO/PEDOT/TFB/ZnMgO/Al) and measured a 1.5 eV energy offset for electron injection into the TFB. The TFB device's current density (J-V curves not shown here) is much higher than that of the device with the QRs, confirming that the electron injection is much faster, even without QRs. The EL spectra of the TFB device compared to QR-LEDs plotted in Figure 2(d) confirm the recombination that occurred in TFB and QRs devices at the same voltage. The electron leakage with path 2 is highly efficient; the energetic disorders present near the LUMO level of the TFB are illustrated with dotted lines in favor of the electron transfer. The tail states of the disorders expand into the band gap, which gives rise to thermally activated hopping transport. $V \gg V_T$, at this stage, the electrons get sufficient energy to overcome the barrier of 1.2 eV and are injected into the TFB, as shown in Figure 3 (d), confirming the electron leakage in both ways. From this, we can conclude that electron leaks with path 1 is highly efficient at a lower bias, while at a higher bias, both paths contribute to electron leakage.

Suppressing the electron leakage into HTL

To suppress electron leakage and parasitic emission from the HTL, it is beneficial to consider an HTL with a shallower LUMO and less energetic disorders. we considered HTLs, including poly((9,9-dioctylfluorenyl -2,7-diyl)-alt-(9-(2-ethylhexyl)-carbazole-3,6-diyl)) (PF8Cz), and Poly(9-vinylcarbazole) (PVK). PF8Cz has less energetic disorders than the TFB and has 0.22 eV shallower LUMO. Similarly, PVK has an even shallower LUMO than PF8Cz and a 0.4 eV deeper HOMO than both TFB and PF8Cz. When turned on, devices with PF8Cz and PVK had much lower leakage currents than TFB and did not show parasitic emission. However, PF8Cz exhibited parasitic emission at 3.2 V, while PVK did so at 6 V, with PVK's emission significantly less than TFB and PF8Cz. PVK is an effective electron-blocking layer, but its hole mobility is only half that of TFB and PF8Cz. Improving hole injection while preventing electron leakage is crucial to enhance device performance. A double-hole transport layer using PF8Cz/PVK stacks was implemented to reduce electron leakage and increase the hole injection.

Device results

Figure 4 presents the results for the green QR-LED device. Using a double-hole transport layer significantly improved the device's current, as shown in Figure 4(a). Additionally, the performance

metrics in Figures 4(b), 4(c), and 4(d) showed remarkable enhancements: luminance increased from 250,000 to 320,000 cd/m^2 , EQE improved from 15.2% to 19.4%, and CE rose from 55 to 72 cd/A . These values represent the highest recorded metrics for green QR-LEDs. Additionally, the device exhibited a T50 lifetime of 10,010 hours at an operating level of 100 cd/m^2 .

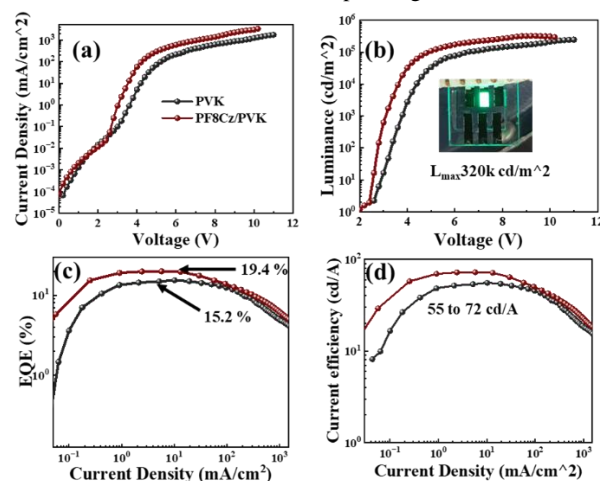


Figure 4. Green QR-LEDs performance with the optimized device (a) current density-voltage, (b) luminance-voltage (insert the emitting green QR-LEDs device), (c) EQE-current density, and (d) current efficiency-current density.

3. Conclusion

We synthesized green QRs with a high QY of over 90% and incorporated them into QR-LEDs. However, electron leakage from the QRs to HTL led to parasitic emission and shifted the electron-hole recombination away from the QRs, negatively impacting device performance. We systematically analyzed the leakage mechanisms based on different device structures to address this. By eliminating charge leakage paths and optimizing the device structure to enhance hole injection, the QR-LEDs achieved record-breaking performance metrics: EQE of 19.4%, CE of 72 cd/A , and luminance of 320,000 cd/m^2 . These figures represent the highest recorded values for green QR-LEDs.

4. Acknowledgements

This work is supported by the Research Grants Council (RGC) of Hong Kong SAR (Nos. 26202019 and 16205623), an Innovation and Technology Commission (ITC) grant, ITS/059/22MX, and the funding for The State Key Laboratory of Advanced Displays and Optoelectronics Technologies

5. References

- Colvin VL, Schlamp MC, Alivisatos AP. Light-emitting diodes made from cadmium selenide nanocrystals and a semiconducting polymer. *Nature*. 1994 Aug 4;370(6488):354-7.
- Coe S, Woo WK, Bawendi M, Bulović V. Electroluminescence from single monolayers of nanocrystals in molecular organic devices. *Nature*. 2002 Dec 19;420(6917):800-3.
- Qian L, Zheng Y, Xue J, Holloway PH. Stable and efficient quantum-dot light-emitting diodes based on solution-processed multilayer structures. *Nature photonics*. 2011 Sep;5(9):543-8.

5-3 / K. Mallem • Distinguished Student Paper

- Liao Z, Mallem K, Prodanov MF, Kang C, Gao Y, Song J, Vashchenko VV, Srivastava AK. Ultralow roll-off quantum dot light-emitting diodes using engineered carrier injection layer. *Advanced Materials*. 2023 Nov;35(47):2303950.
- Kim WD, Kim D, Yoon DE, Lee H, Lim J, Bae WK, Lee DC. Pushing the efficiency envelope for semiconductor nanocrystal-based electroluminescence devices using anisotropic nanocrystals. *Chemistry of Materials*. 2019 Apr 22;31(9):3066-82.
- Frischeisen J, Yokoyama D, Adachi C, Brütting W. Determination of molecular dipole orientation in doped fluorescent organic thin films by photoluminescence measurements. *Applied Physics Letters*. 2010 Feb 15;96(7).
- Kang C, Prodanov MF, Gao Y, Mallem K, Yuan Z, Vashchenko VV, Srivastava AK. Quantum-Rod On-Chip LEDs for Display Backlights with Efficacy of 149 lm W⁻¹: A Step toward 200 lm W⁻¹. *Advanced Materials*. 2021 Dec;33(49):2104685.
- Mallem K, Prodanov MF, Dezhang C, Marus M, Kang C, Shivarudraiah SB, Vashchenko VV, Halpert JE, Srivastava AK. Solution-processed red, green, and blue quantum rod light-emitting diodes. *ACS Applied Materials & Interfaces*. 2022 Apr 13;14(16):18723-35.
- Kang C, Prodanov MF, Song J, Mallem K, Liao Z, Vashchenko VV, Srivastava AK. Robust, Narrow-Band Nanorods LEDs with Luminous Efficacy > 200 lm/W: Next-Generation of Efficient Solid-State Lighting. *Small*. 2024 Mar 27;2311671.
- Mallem K, Prodanov MF, Liao Z, Kang C, Vashchenko VV, Srivastava AK. 83-3: Electron Transportation Engineering for Record High External Quantum Efficiency of 16.8% for Quantum Rod Light-Emitting Diodes. *InSID Symposium Digest of Technical Papers 2023 Jun (Vol. 54, No. 1, pp. 1170-1173)*.
- Zhang Q, Zhang D, Liao Z, Cao YB, Kumar M, Poddar S, Han J, Hu Y, Lv H, Mo X, Srivastava AK. Perovskite Light-Emitting Diodes with Quantum Wires and Nanorods. *Advanced Materials*. 2024;2405418.
- Mallem K, Prodanov MF, Liao Z, et al. Quantum rod light emitting diodes: Suppressing leakage current and improving external quantum efficiency. *Nano Research*, 2024, <https://doi.org/10.26599/NR.2025.94907071>
- Zeng Y, Liu X, Liu Y, Chen W, Liu F, Li H. 22% Record Efficiency in Nanorod Light-Emitting Diodes Achieved by Gradient Shells. *Advanced Materials*. 2024 May;36(19):2310705.
- Liao Z, Prodanov MF, Mallem K, Kang C, Song J, Bhadra D, Srivastava AK. 44-3: High Efficiency and Brightness Quantum Rods Light Emitting Diode. *InSID Symposium Digest of Technical Papers 2024 Jun (Vol. 55, No. 1, pp. 585-587)*.
- Mallem K, Liao Z, Prodanov MF, Song J, Bhadra D, Gavara RR, Srivastava AK. 28-4: Positive Aging Resulted in Highly Efficient Blue Quantum Rod Light Emitting Diodes. *InSID Symposium Digest of Technical Papers 2024 Jun (Vol. 55, No. 1, pp. 360-363)*.